REVIEW: STRUCTURAL STAINLESS STEEL SEISMIC FORCE-RESISTING SYSTEMS

F. Meza[1], N. Baddoo[2], B.R. Baer[3], B. Manley[4], B.W. Schafer[5]

ABSTRACT

This paper presents an overview of design considerations for structural stainless steel seismic force-resisting systems (SFRS). While stainless steel is widely utilized for its corrosion resistance and aesthetic appeal in various structural applications, its seismic design in the U.S. remains underdeveloped due to the absence of dedicated U.S. design standards. This research addresses the mechanical properties, cyclic performance, and seismic behavior of austenitic and duplex stainless steels, highlighting their significant strain hardening, ductility, and toughness under cyclic loading. Comparative studies with carbon steel indicate the potential for stainless steel SFRS to achieve equivalent or superior seismic performance. Preliminary recommendations for adapting existing seismic design provisions, such as ASCE 7 and AISC 341, to stainless steel structures are proposed, covering material factors, width-to-thickness and stability bracing requirements, and system-specific seismic design parameters. These guidelines aim to bridge existing gaps and encourage broader adoption of stainless steel in seismic applications, while identifying future research needs for comprehensive standards development.

1. INTRODUCTION

Stainless steels are generally used in applications requiring a high level of corrosion resistance, for example structures located in aggressive environments (e.g. by the coast or splashed by deicing salts). Applications where maintenance needs to be minimized or protective coatings avoided are also a common reason for using stainless steel (e.g. structures in nuclear installations, or bridges over railways). The majority of applications of structural stainless steels are found in industrial structures for water/wastewater treatment, pulp and paper, nuclear, biomass, chemical, pharmaceutical, and food and beverage industries. These applications include platforms, structures in 'clean' rooms, enclosures and support systems for pipework and equipment, as well as walkways, tanks and tank supports. Applications of stainless steels in building structures usually have an aesthetic focus, such as exposed canopies and entrance structures, although there are also unseen applications such as cladding support systems. Stainless steel applications are generally classified as non-building structures or nonstructural components. AISC Design Guide 27, *Structural Stainless Steel* gives more information on applications of structural stainless steels (Baddoo and Meza, 2022) and Figure 1 to Figure 4 illustrate examples of the use of structural stainless steels.

[1] Steel Construction Institute, UK, <F.Meza@steel-sci.com>
[2] Steel Construction Institute, UK, <n.baddoo@steel-sci.com>
[3] Consulting Structural Engineer, US, <baeroffice@att.net>
[4] American Institute of Steel Construction, US, <manley@aisc.org>
[5] Department of Civil and Systems Engineering, Johns Hopkins University, <schafer@jhu.edu>

Figure 1 Stainless steel walkways, platforms, floors and supports at a paper mill.

Figure 2 Stainless steel support tower at the Vogtle Nuclear Power Plant Units 3 & 4.
© Premier Industrial/Westinghouse

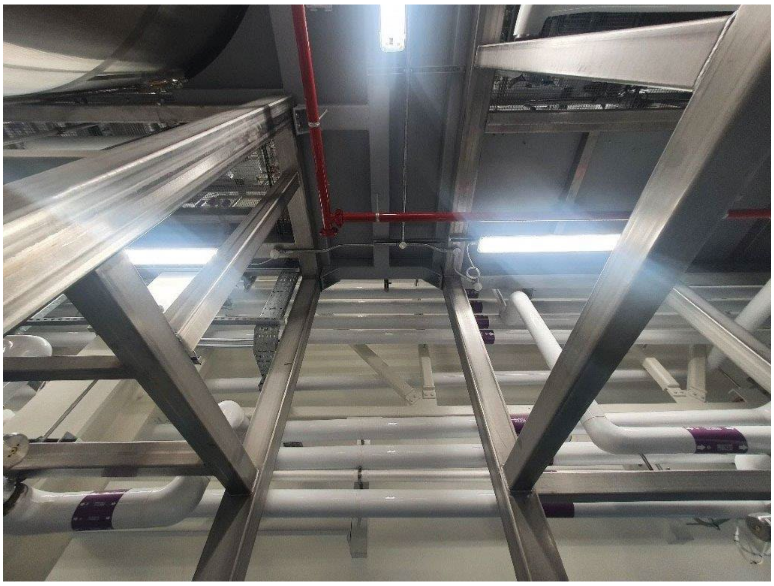

Figure 3 Stainless steel maintenance platform in a 'clean room' in a biopharmaceutical product plant.

© PM Group

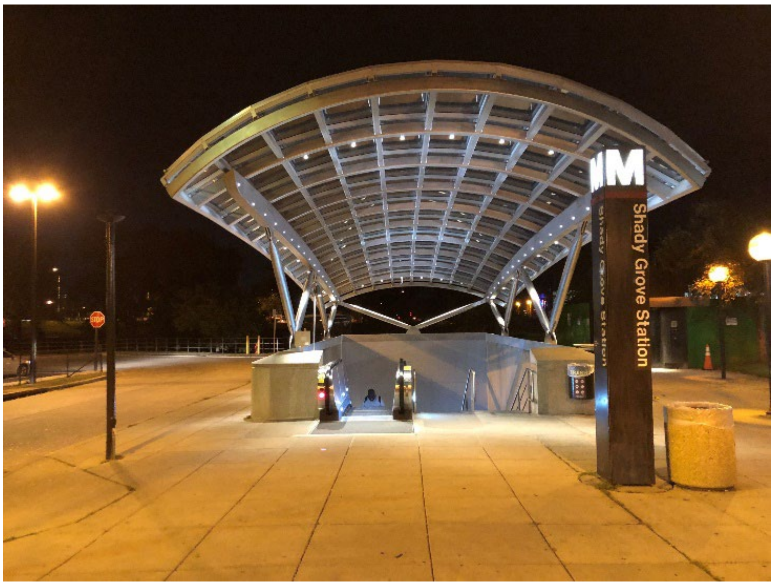

Figure 4 Stainless steel canopy over the entrance to Shady Grove underground station - one of 40 similar canopies on the Washington, DC Metro.

© Chattanooga Boiler and Tank Company

The most common type of stainless steels used in construction are austenitic stainless steels. They provide a useful combination of corrosion resistance, forming, and fabrication properties with design strength of approximately 205 MPa (30 ksi). The basic chromium-nickel austenitic alloys, S30400 and S30403 (according to ASTM A240/A240M, but widely known as 304 and 304L) are suitable for rural, urban and light industrial sites. The chromium-nickel-molybdenum austenitic alloys S31600 and S31603 (widely known as 316 and 316L) are more highly alloyed alloys and will perform better in marine and many industrial environments. The S30403 and S31603 alloys are low-carbon versions of the S30400 and S31600 alloys, respectively, with a reduced risk of sensitization to intergranular corrosion in the heat affected zones of welds of these stainless steels.

Duplex stainless steels are mostly specified where their higher strength can be utilized. The duplex alloy S32205 (widely known as 2205) has a yield strength of around 450 MPa (65 ksi), good wear resistance and very good resistance to stress corrosion cracking. In addition, the newer lean duplex alloys offer high strength combined with a leanly alloyed chemical composition, making them less expensive. S32101, for example, has a yield (proof) strength of 450 MPa (65 ksi), and a corrosion resistance between that of austenitic alloys S30400 and S31600.

Sheet, plate, bar and tubular products are all available in the stainless steel alloys mentioned previously. A range of hot rolled or welded structural sections (I-sections, angles, channels, tees, hollow sections) are stocked in austenitic stainless steels but duplex stainless steels usually require special orders. Both conventionally arc welded sections and laser welded sections are available.

AISC 370-21, *Specification for Structural Stainless Steel Buildings* (AISC, 2021) was released in 2021 and covers the design, fabrication, and erection of building-type structures made of austenitic and duplex structural stainless steels. The design provisions cover hot-rolled and welded sections, as well as cold-formed hollow structural sections. Ten austenitic stainless steel alloys and nine duplex stainless steel alloys are included. There are many other stainless steel alloys, but they are not used for structural applications.

The scope of AISC 370 does not cover stainless steel structures that are subject to seismic loads, and there is currently no U.S. design code that covers the design of these structures. This can greatly hinder the use of structural stainless steels in the U.S., especially in high seismic regions.

This review paper provides a summary of relevant research on the seismic performance of structural stainless steel and gives preliminary recommendations for the development of design rules for stainless steel structures subject to seismic loads that are aligned with the provisions given in ASCE 7 (ASCE, 2022) and AISC 341 (AISC, 2022b) for carbon steel seismic force-resisting systems (SFRS). These recommendations are proposed for use by engineers until such time as formal guidance is incorporated in the standards. The paper also identifies known holes and gaps for future action.

2. BACKGROUND

2.1. Structural Stainless Steel Mechanical Properties

The design of structural stainless steels differs slightly from the design of carbon steel structures primarily due to the difference in their stress-strain behavior. Whereas carbon steel typically exhibits linear elastic behavior up to the yield stress and a plateau before strain hardening, stainless steels have a more rounded response with no well-defined yield stress. Due to the rounded stress-strain characteristics exhibited by stainless steels, their ‘yield' strength is generally quoted in terms of the 0.2% proof strength. i.e. the proof strength at an offset permanent strain of 0.2%. Austenitic and duplex stainless steels exhibit significant strain hardening and ductility. For austenitic stainless steels the tensile-to-yield stress ratio (F_u/F_y) is around 2.1 and the elongation at fracture is at least 40%, while for duplex stainless steels F_u/F_y is typically 1.4 and the elongation at fracture is generally larger than 25%. The inelastic behavior of typical austenitic and duplex stainless steels is compared in Figure 5 against the typical behavior of a Grade 50 carbon steel (Baddoo and Meza, 2022), while the mechanical properties of typical austenitic and duplex stainless steels are summarized in Table 1. A comprehensive list of the austenitic and duplex stainless steel alloys that are used in structural applications, including their mechanical properties, is included in the Commentary to AISC 370 (AISC, 2021).

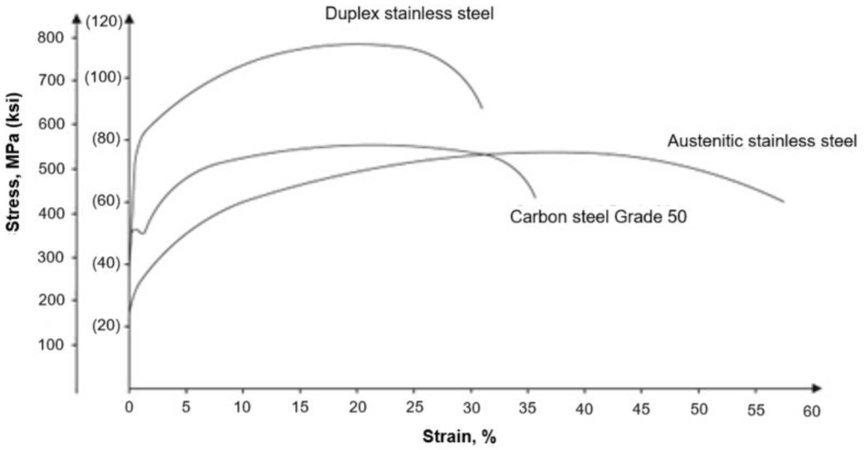

Figure 5 Typical stress-strain curves for stainless steel and carbon steel.

Table 1 Mechanical properties of typical stainless steels.

Alloy family	*E*, MPa (ksi)	F_y, MPa (ksi)	F_u, MPa (ksi)	ε_u, %
Austenitic	193000 (28000)	205 (30)	515 (75)	>40
Duplex	200000 (29000)	450 (65)	655 (95)	>25

Stainless steels also exhibit equivalent or superior toughness compared to carbon steels. While duplex stainless steels exhibit a ductile-to-brittle temperature transition behavior comparable to carbon steel, the toughness of austenitic stainless steels is significantly superior over a wide range of temperatures. There is no ductile-to-brittle transition for austenitic stainless steels down to cryogenic temperatures. Austenitic and duplex stainless steels also show good weldability, i.e. welded joints show good strength, ductility and toughness.

2.2. Structural Stainless Steel Connections

Austenitic stainless steels are weldable, and AWS D1.6/D1.6M, *Structural Welding Code – Stainless Steel* (AWS, 2017) provides prequalified base metals, prequalified filler metals, and prequalified joints. Duplex stainless steels can be readily welded; however, there are no prequalified base metals, no prequalified filler metals, and no prequalified joints in AWS D1.6/D1.6M for duplex stainless steels. It is expected that these will be added to AWS D1.6/D1.6M in a later revision.

Filler metals for welding austenitic stainless steels can achieve Charpy V-notch (CVN) toughness in excess of 80 J (60 ft-lbf) at temperatures as low as -196°C (-320°F), while for duplex stainless steels, despite the lack of prequalification, filler metals can achieve CVN toughness greater than 40 J (30 ft-lbf) at -40°C (-40°F) (Voestalpine, 2013).

Corrosion resistance is often the primary consideration when selecting a filler metal for welding both austenitic and duplex stainless steels. This augments the usual design of welds for carbon steel connections, where strength is the primary consideration. Overmatching still remains common practices —when the connected parts are made of the same stainless steel alloy, the strength of the filler metal is specified to be greater than that of the connected parts.

Note, to achieve the required corrosion resistance of the weld metal in connections between stainless steel and carbon steel, the filler metal usually should have a higher concentration of the alloying elements than the base metal (referred to as "over-alloyed"). This is to account for dilution of the filler metal as it mixes with the molten base metal.

For bolted connections, the provisions in AISC 370 for bearing and tearout strength differ from those in AISC 360, with the bearing strength for stainless steel being lower due to the ductility and strain hardening characteristics of stainless steels. Also, when stainless steel is connected to carbon steel through a bolted connection, the dissimilar metals may need to be electrically isolated from one another to avoid the risk of galvanic corrosion if moisture infiltration or condensation occurs within the joint. This is usually achieved by using insulating washers and bushings to prevent contact between the bolt and plates. Alternatively, an insulating and sealing material can be used underneath the washers and the perimeter of the joint subsequently sealed to prevent moisture. For slip-critical connections, separation can be achieved by ensuring adequate coating is applied to the carbon steel part.

2.3. International Structural Stainless Steel Seismic Design Standards and Practice

In Japan, the seismic design of stainless steel and carbon steel structures is identical (Tada et al., 2003). For most steel buildings less than 31 meters (100 feet) tall, the seismic design requires that the structure remains elastic under a moderate intensity earthquake, while for taller buildings up to 60 meters (200 feet), the structure also has to be designed to resist a major earthquake allowing controlled damage in the structure. For buildings taller than 60 meters (200 feet), the seismic design for the moderate intensity and major earthquake is based on time history dynamic analyses. The response modification coefficients that are used when allowing controlled damage of the structure are the same for carbon steel and stainless steel structures; however, these coefficients can be around half of those used in the U.S. for braced frames and moment resisting frames of carbon steel construction (Tada et al., 2003). When designing the energy dissipating members according to the Japanese seismic design code, the strain hardening exhibited by the material is not considered.

The Chinese design code for stainless steel structures (CECS, 2015) adopted the seismic design rules given in GB 50011, the *Code for Seismic Design of Buildings* (GB/GBT, 2010). The overall Chinese seismic design approach is generally more simplified than the U.S. approach, primarily due to the way in which the seismic design forces are calculated which does not capture the different levels of inelastic deformation that different types of structures can develop, essentially assuming a response modification coefficient R, (R-factor), equal to 3 for all of them. However, based on recent research, the next revision of the Chinese stainless steel design code, expected in 2025, will permit the use of different R factors depending on the type of structure —but it is not known if specific rules for stainless steel will exist.

Most European countries are not susceptible to high intensity earthquakes. The European code for seismic design of steel structures is EN 1998 (CEN, 2004). For the design of stainless steel structures, EN 1993-1-4 (CEN, 2015) gives supplementary rules that need to be applied in order to extend the rules given in the design codes for carbon steel; however, EN 1993-1-4 does not give supplementary rules for seismic (i.e. to EN 1998) .

2.4. US Structural Stainless Steel Design Standards and Practice

The new AISC 370 (AISC, 2021) has enabled austenitic and duplex stainless steel structures to be efficiently designed with provisions that are tailored to the particular characteristics of these stainless steel alloy families; however, despite the favorable ductility, toughness, and weldability of stainless steels, there are currently no U.S. standards that cover the design of welded and hot-rolled structural stainless steel seismic force resisting systems (SFRS), and therefore their design must be based on conservative assumptions. ASCE 7 (ASCE, 2022) gives seismic design parameters for light-weight structures made of cold-formed stainless steel. These seismic design parameters are identical to those given for light-weight structures made of cold-formed carbon steel.

Prior to the publication of AISC 370 in 2021, seismic design of stainless steel structures was commonly completed assuming a response modification coefficient $R = 3$ for the seismic loads, with the strength of the structure calculated using the design provisions given in AISC 360 (AISC, 2016) for carbon steel buildings, but with the modifications recommended in Design Guide 27, *Structural Stainless Steel* (Baddoo, 2013) for stainless steel buildings. This design approach relies on an assumed performance similar to "ordinary" carbon steel structural systems —and typical carbon steel building framing applications. Structural stainless steel systems have attributes that suggest better seismic performance is possible (ductility, toughness), but others, such as their unique framing applications in industrial structures that, lead to questions regarding similarity to "ordinary" performance. Some stainless steel structures that need to remain operative after an earthquake, such as nuclear power plants or water treatment facilities certainly require more care than a simplified $R = 3$ approach, and some nonbuilding-type of structures may need to be designed using an R-factor smaller than 3.

Although AISC 370 does not cover the design of stainless steel structures that are subject to seismic loads, this specification refers to ASCE 7, Section 12.2.1.1 as a way of providing some guidance to the engineer for the seismic design requirements of stainless steel structures. However, the requirements given in ASCE 7, Section 12.2.1.1 put all the responsibility on the engineer to develop and prove their own seismic design criteria for stainless steel structures. As a result, even the design of structures that are subject to low seismic forces becomes an impractically complicated endeavor. An improved and workable standard of care for seismic design of structural stainless steel systems in the U.S. is needed.

3. RELEVANT RESEARCH ON STRUCTURAL STAINLESS STEEL SFRS

3.1. Overstrength of Structural Stainless Steels

The overstrength (expected greater than nominal) of austenitic and duplex stainless steel alloys was investigated by Meza et al. (2024), where overstrength material factors for the yield and ultimate tensile strength for use in reliability calculations for AISC 370 were proposed. These material factors were derived by analyzing material data provided by stainless steel producers, encompassing a wide range of stainless steels and material thicknesses. The overstrength distributions reported in that study are illustrated in Figure 6, which shows that austenitic stainless steel alloy overstrength is approximately a normal distribution, and duplex stainless steel alloys have a bi-modal overstrength distribution. This bi-modal distribution, which is not unique to stainless steel, can be attributed to several sources of bias introduced when assembling the data, as explained in Meza et al. (2024). To address this issue, Meza et al. gradually removed data points with the largest overstrength from the assembled data until the distribution of the lower tail followed the assumed normal distribution, as shown in Figure 6. For seismic design; however, it is the upper tail of the distribution that is of relevance. Also, given the wide dispersion of the distribution, especially for the yield strength, the mean may not give a sufficiently safe estimate of the expected strength needed for capacity-based design, and therefore, the use of a larger fractile is explored in this paper (see Section 1.1).

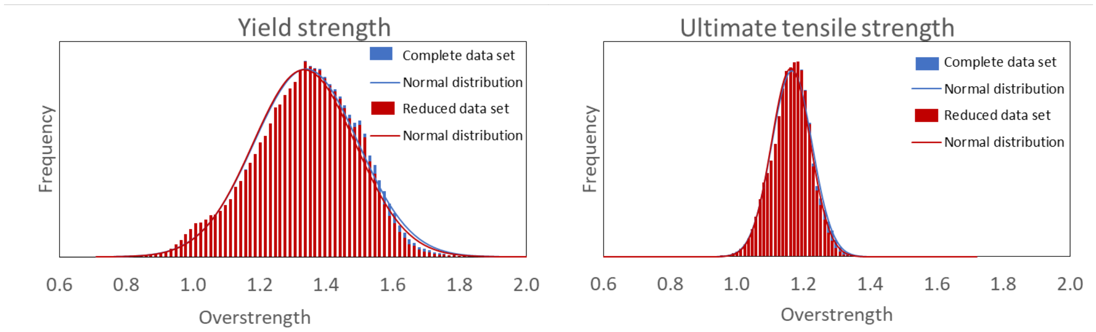

(a) Austenitic stainless steel

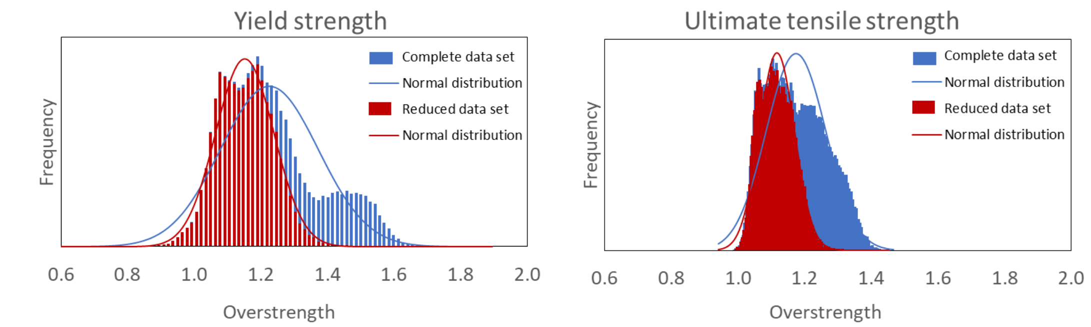

(b) Duplex stainless steel

Figure 6 Overstrength distribution of stainless steels (Meza et al., 2023).

3.2. Cyclic Material Characteristic of Structural Stainless Steels

There has been a large amount of research, particularly in the past few years, dedicated to investigating the hysteretic behavior of structural stainless steels under large cyclic strains (Dutta et al., 2010; Nip et al., 2010a; Wang et al., 2014; Zhou and Li, 2016; Baiguera et al., 2019; Chang et al., 2019; Yin et al., 2019; Annan and Beaumont, 2020; Lazaro and Chacon, 2022). Most of this work has focused on austenitic stainless steel alloys (e.g. S30400/S30403, S30408, S31600, S31603 and S31653); however, research on duplex and lean duplex stainless steel alloys (e.g. S32205 and S31803 and S32101) has also been reported (Chang et al., 2019; Baiguera et al., 2019; Zhou and Li, 2016).

These studies have shown that austenitic stainless steels exhibit significantly greater levels of cyclic hardening than carbon steel, whereby the strength of the steel increases with subsequent loading cycles. Figure 7 compares the cyclic and monotonic stress-strain curve obtained from coupons taken from plates made of austenitic stainless steel S30400/S30403 and carbon steel Grade 350WT (Canadian Grade used in bridges, similar to Grade 50), with $F_y = 350$ MPa (50 ksi), as reported by Annan and Beaumont (2020). For duplex and lean duplex stainless steels, tests carried out by Chang et al. (2019) on S32205 coupons and tests carried out by Zhou and Li (2016) on S32101 have shown cyclic hardening to be less significant than for austenitic stainless steels. A comparison of the cyclic (envelope) and monotonic stress-strain behavior for austenitic (S30400) and lean duplex (S21010) stainless steel is provided in Figure 8 for different product forms, i.e. hot-rolled plate, cold-rolled sheet, and finished cold-formed hollow structural sections (Zhou and Li, 2016).

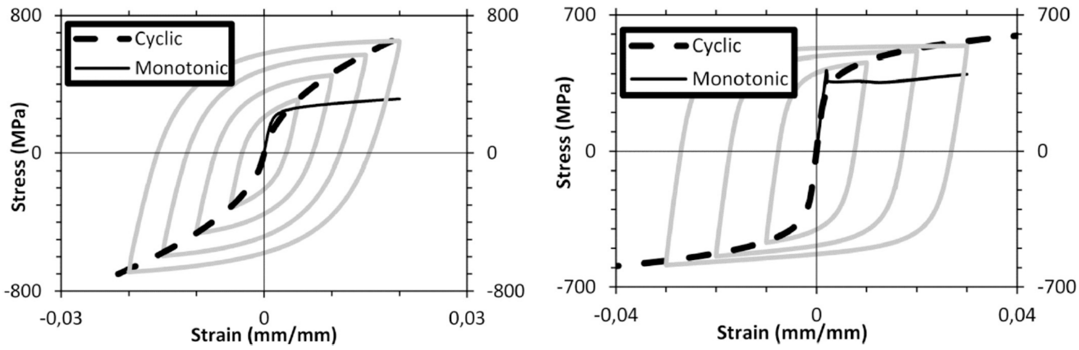

(a) Austenitic stainless (b) Carbon steel

Figure 7 Cyclic and monotonic stress-strain comparison for: a) austenitic stainless steel S30403; b) carbon steel Grade 350WT (Annan and Beaumont, 2020).

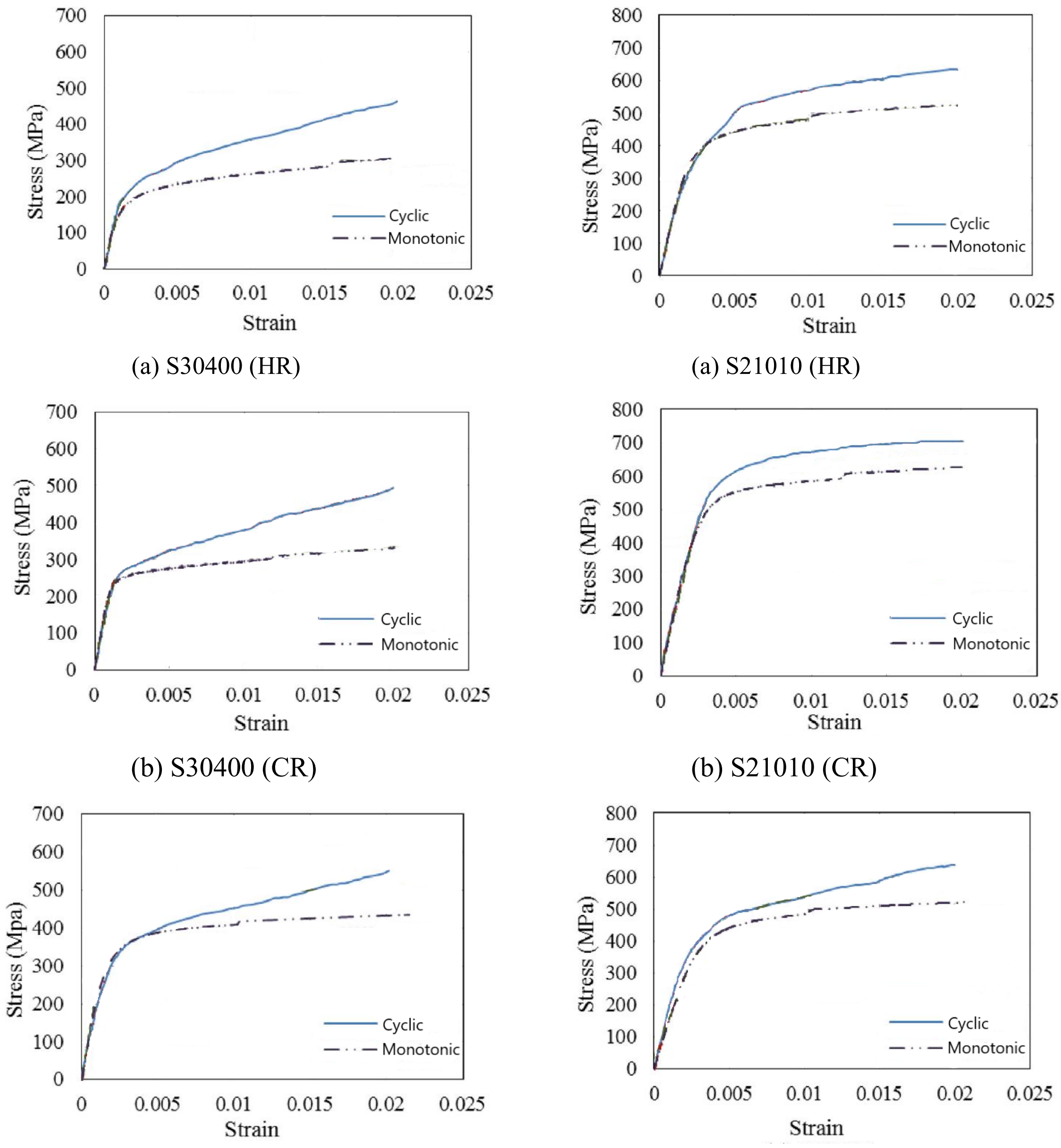

(a) S30400 (HR) (a) S21010 (HR)

(b) S30400 (CR) (b) S21010 (CR)

(c) S30400 (CF) (c) S21010 (CF)

Figure 8 Cyclic and monotonic stress-strain comparison for austenitic (S30400) and duplex (S21010) stainless steel in different product forms: a) Hot rolled plate (HR); b) Cold-rolled sheet (CR); c) Finished cold-formed structural hollow section (CF) (Zhou and Li, 2016).

The effect of cyclic hardening has been shown to be particularly important for strains larger than around 1.0%, and increases significantly as the cyclic strain increases, with the material being able to reach stresses even greater than the ultimate tensile strength obtained from a monotonic test. At 2.0% strain, the cyclic stresses of austenitic stainless steels have been reported to be, after 50 cycles, up to 2.1 times the stress at 2.0% strain recorded from a monotonic test, with the value reported corresponding to that at half the fatigue life of the specimen (Annan and Beaumont, 2020). For duplex and lean duplex stainless steels, on the other hand, tests carried out by Chang et al. (2019) and Zhou and Li (2016) have shown the cyclic hardening at 2% strain to be around 1.12 to 1.27 times the corresponding monotonic stress.

Figure 9 compares the progression of cyclic hardening as a function of the number of cycles obtained from stainless steel and carbon steel coupons subject to cyclic strains of up to 1% and 2%. The figure shows that while for carbon steel, the cyclic stress-strain characteristic stabilizes within the first few cycles, for austenitic stainless steels strained at 2% the cyclic stress-strain characteristics continue to increase; however, for strains of up to 1%, the cyclic hardening evolution of austenitic stainless steel resembles that of carbon steel, with some additional increase in cyclic hardening, but only after 100 cycles. The cyclic hardening evolution of duplex stainless steel appears similar to that of carbon steel even when the material is strained at 2%. However, more data is needed to confirm this.

The implication of cyclic hardening is that the inelastic behavior of the material becomes stiffer as the inelastic loading cycles progress. Therefore, if the energy dissipating components of a SFRS are made of austenitic stainless steels, and are designed without consideration of this behavior, this may lead to an excessive increase in strength demand on the member end-connection and adjacent elements that are required to remain elastic. For example, the larger cyclic hardening could impact the design of columns as well as the design of column-to-foundation.

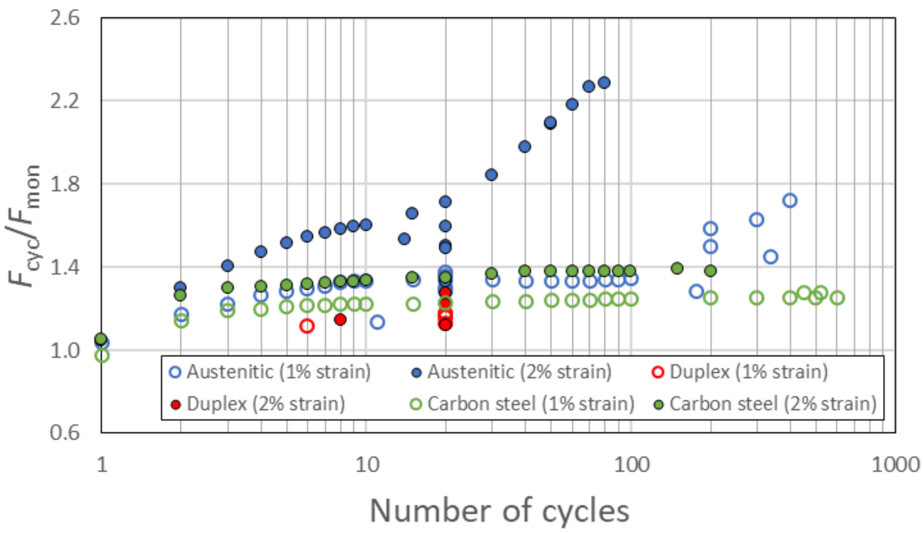

Figure 9 Comparison of cyclic hardening evolution for stainless steels and carbon steel recorded from tensile coupons in the reviewed literature.

Regarding the fatigue life of structural stainless steels subject to large strain cycles, different observations have been reported. Nip et al. (2010a) reported that specimens taken from cold-formed hollow structural sections made of austenitic stainless steels and carbon steel exhibit similar strain-life relationship when subject to strains of up to 15%, as shown in Figure 10, while Colin et al. (2011) has reported that austenitic stainless steels exhibit better low-cycle fatigue life than carbon steel. On the other hand, the experimental work by Annan and Beaumont (2020) revealed that carbon steel Grade 350WT has a longer low-cycle fatigue life than austenitic stainless steel S30403. The shorter low-cycle fatigue life for the austenitic stainless steel alloy was attributed to the strain-induced martensitic transformation exhibited by the material. However, Annan and Beaumont (2020) also pointed out that the variability of the low cycle fatigue of austenitic stainless steels plays a significant role, and therefore more research is needed to explain this variability. It is worth pointing out that the specimens tested by Annan and Beaumont (2020) exhibited fatigue life of more than 100 cycles, which is larger than the number of cycles expected during an earthquake, as the specimens were only subject to strains of up to 2%. No equivalent work appears to have been carried out on duplex stainless steels.

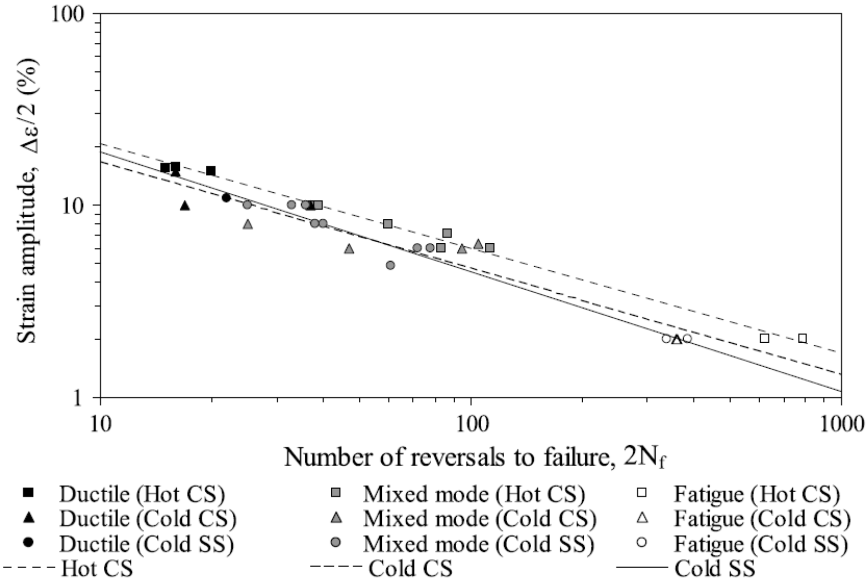

Figure 10 Strain-life relationship and fracture modes of bending test specimens made of hot-rolled carbons steel (S355J2H), cold-formed carbon steel (S235JRH) and cold-formed austenitic stainless steel S30400/S30403 (Nip et al., 2010a).

3.3. Braces and Members

Tests on cold-formed austenitic stainless steel (S30400) rectangular hollow structural sections (HSS) subject to cyclic major axis bending have been reported by Gonzalez de Leon et al. (2022). The specimens were tested as cantilever beams bolted at one end and loaded following the loading protocol specified in AISC 341. The specimens were designed to fail away from the bolted connection. HSS with different width-to-thickness ratios were investigated. The width-to-thickness ratios of these specimens is compared in Table 2 against the limiting values given in AISC 341 and AISC 370, which shows that only Section 2 did not meet the limiting width-to-thickness ratio for highly ductile members given in AISC 341. The specimens with Section 2 exhibited local buckling before failure, as revealed by the gradual strength degradation in their hysteretic behavior before fracture shown in Figure 11. However, the occurrence of local buckling did not prevent the section from attaining its plastic moment capacity, which is indicated by $F_{pl} = M_{pl}/L = F_{y,avg}Z_x/L$, and did not have a significant effect on the fracture life of the specimen, as all tested beams were able to sustain a similar number of cycles before fracture of the section corners (>39 cycles).

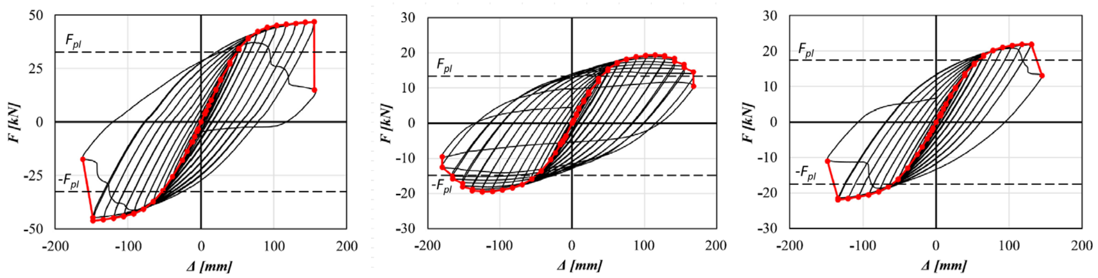

(a) (b) (c)

Figure 11 Hysteretic response of representative beam with: a) Section 1; b) Section 2; c) Section 3 (Gonzalez de Leon et al., 2022).

Table 2 Limiting width-to-thickness ratios for the most slender element of cold-formed HSS tested in the reviewed literature.

Research group	Section[a]	Steel	*H* (mm)	*B* (mm)	*t* (mm)	r_o (mm)	b/t	AISC 341		AISC 370	Local buckling?
								λ_{hd}	λ_{md}	λ_p	
Gonzalez de Leon et al. (2022)	1	304	120.0	80.0	6.0	20.1	6.6	9.9	18.0	21.1	No
	2	304	99.8	80.2	3.9	12.6	14.1	11.0	20.0	23.5	Yes
	3	304	120.14.73	41.1	3.9	12.1	4.3	9.7	17.6	20.6	No
Nip et al. (2010)	1	S355	60.4	60.3	3.3	6.0	14.9	14.1	16.5	25.4	Yes
	2	S355	40.1	39.9	3.0	4.7	10.3	13.9	16.3	25.1	Yes
	3	S235	59.9	59.8	2.8	6.8	16.8	15.6	18.2	28.0	Yes
	4	S235	40.4	40.3	3.8	7.3	6.9	14.4	16.9	25.9	No
	5	S235	40.1	40.0	2.8	5.8	10.2	14.1	16.5	25.4	Yes
	6	304/304L	60.6	60.3	2.8	5.5	17.8	13.2	15.4	23.7	Yes
	7	304/304L	50.2	50.0	2.8	3.8	15.5	12.3	14.4	22.2	Yes
	8	304/304L	60.1	40.0	2.8	4.3	18.8	12.3	14.3	22.1	Yes[b]
Zhou et al. (2018)	1	304	60.3	60.3	3.9	5.5	12.8	11.3	13.2	20.3	No
	2	304	60.3	60.3	1.9	2.5	29.6	12.9	15.1	23.2	Yes
	3	304	60.3	40.3	3.8	5.5	12.8	11.3	13.2	20.3	No
	4	304	60.3	40.3	1.9	2.4	29.6	12.4	14.5	22.4	Yes
Kim et al. (2021)	1	304	50.2	50.0	3.1	5.0	13.1	12.5	14.6	22.5	No
	2	304	70.2	69.8	3.1	5.0	19.6	12.0	14.0	21.5	Yes
	3	316	50.1	48.8	3.1	5.0	13.1	13.3	15.6	24.0	Yes[b]
	4	316	69.9	69.9	3.0	5.0	19.8	13.9	16.3	25.0	Yes[b]
	5	2101	70.4	70.2	1.6	6.0	36.6	11.9	14.0	21.5	Yes

[a] Specimens with the same section but different lengths were tested.
[b] No local buckling was reported for the longest specimen.
Note:

$\lambda_{hd} = 0.55\sqrt{\frac{E}{F_{y,avg}}}$; $\lambda_{md} = 1.00\sqrt{\frac{E}{F_{y,avg}}}$; $\lambda_p = 1.17\sqrt{\frac{E}{F_{y,avg}}}$ for the beams tested by Gonzalez de Leon et al.

$\lambda_{hd} = 0.65\sqrt{\frac{E}{F_{y,avg}}}$; $\lambda_{md} = 0.76\sqrt{\frac{E}{F_{y,avg}}}$; $\lambda_p = 1.17\sqrt{\frac{E}{F_{y,avg}}}$ for the braces tested by the other researchers.

$F_{y,avg}$ is the average yield strength based on measured material properties obtained from monotonic tensile coupon tests.

Tests on austenitic stainless steel braces subject to cyclic axial loading have been reported by Nip et al. (2010b), Zhou et al. (2018) and Kim et al. (2021). In all these studies, the braces consisted of cold-formed rectangular or square HSS with a maximum slenderness ratio of $6.3\sqrt{E/F_y}$, which is the maximum value permitted by the European seismic design code EN 1998-1 (CEN, 2004), and exhibited global buckling under compressive load. The cyclic load followed the multi-step loading protocol recommended by ECCS (1986), modifications of this loading protocol or the ATC 24 loading protocol, which are illustrated in Figure 12. While the braces tested by Zhou et al (2018) and Kim et al. (2021) covered both stocky and slender cross-sections, the study by Nip et al. (2010b) only focused on HSS with stocky cross-sections. However, none of these specimens satisfied the width-to-thickness limit for highly ductile members given in AISC 341 and local buckling was reported for some specimens, as summarized in Table 2.

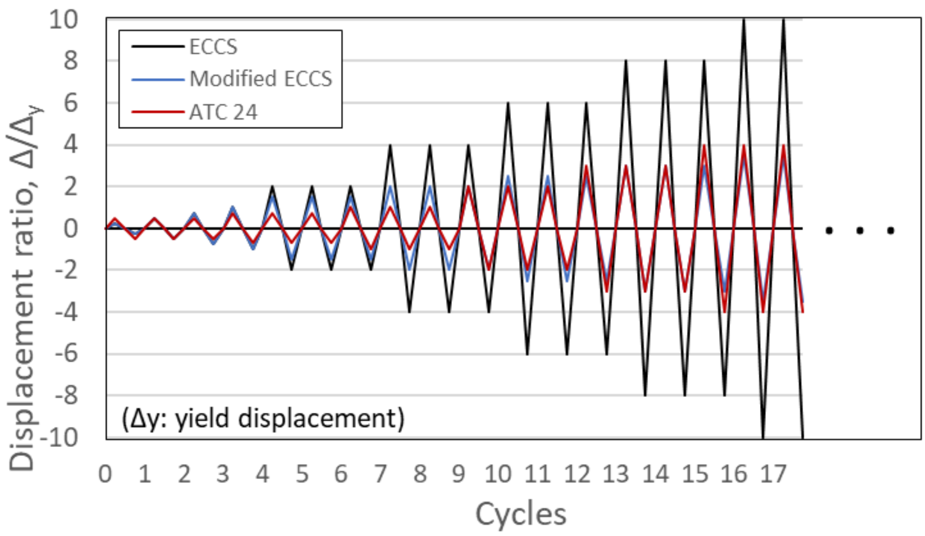

Figure 12 Loading protocols used by Nip et al. (ECCS), Zhou et al. (ECCS and Modified ECCS) and Kim et al. (ATC 24).

In the study by Nip et al. (2010b) the cyclic response of the austenitic braces was compared to that of carbon steel braces. The austenitic stainless steel braces exhibited more pronounced cyclic hardening, which was manifested by a high maximum tensile resistance, and also a less pronounced reduction in the compressive flexural buckling resistance which takes place with successive loading cycles. The latter effect suggests that the 30% rule given in AISC 341 (AISC, 2022b) for calculating the compressive resistance of the braces can be conservatively adopted for stainless steel braces. A numerical investigation by Nip et al. (2010b) also showed that the stainless steel braces were able to sustain a larger number of cycles than the carbon steel braces before fracture. This was partly because stainless steel is able to maintain a higher level of compressive post-yield stiffness (due to strain hardening), thus delaying the occurrence of local buckling, which has a detrimental effect on the fracture life. The energy dissipation of the austenitic stainless steel braces was also found to be similar to that of the carbon steel braces at a given strain amplitude. However, the total energy dissipation of the stainless steel braces was higher due to the larger number of cycles they were able to undergo before fracture. The study by Kim et al. (2021) also included two duplex stainless steel braces; however, their cross-section was slender and their behavior was significantly affected by local buckling (in addition to global buckling), which limited the amount of cyclic and strain hardening they were able to develop.

A comparison of the combined cyclic and strain hardening (F_{cyc}/F_y) achieved by the beams tested by Gonzalez de Leon et al. (2022), and the braces tested Nip et al. (2010), Zhou et al. (2018) and Kim et al. (2021) is illustrated in Figure 13. The figure shows the more pronounced F_{cyc}/F_y exhibited by the austenitic stainless steel braces compared to the carbon steel braces, and how this is limited by global and local instabilities. It is worth pointing out that the amount of cyclic hardening achieved by the members shown in Figure 13 is smaller than that obtained from tensile coupons in Figure 9, even when instabilities are prevented (as was the case in some of the specimens tested by Gonzalez de Leon et al. (2022)). This can be explained by the non-uniform strain distribution within the cross-section of these members.

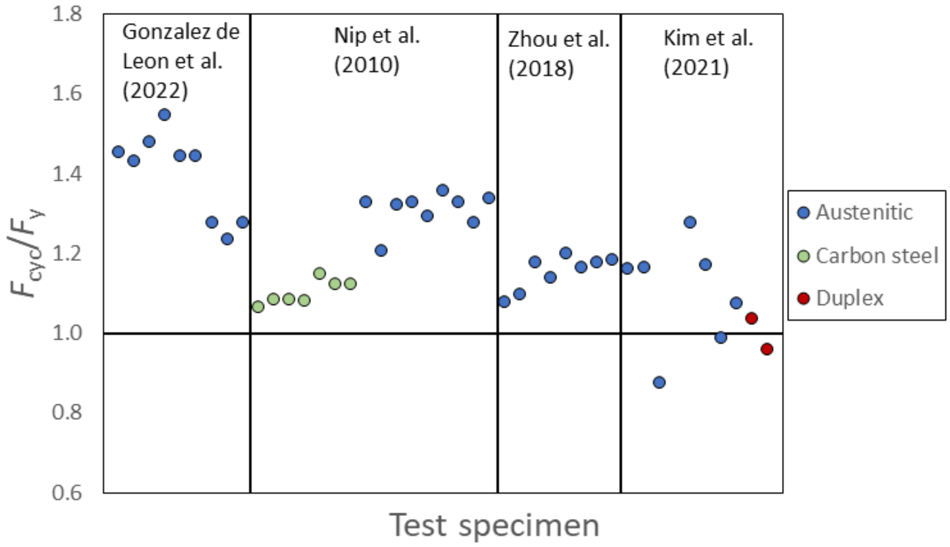

Figure 13 Comparison of combined cyclic and strain hardening for stainless steels and carbon steel tubular members reported in the reviewed literature.

Lanning et al. (2016) reported the only cyclic tests so far on buckling-restrained braces (BRB) made of austenitic stainless steel S30400/S30403. The braces were fabricated by CoreBrace, LLC, and were tested in the United States. The BRBs were subject to different consecutive loading protocols (Proof protocol, near-fault protocol and the AISC protocol for BRBs). The austenitic BRBs were shown to be resilient in inelastic deformation and energy dissipation capabilities, showing no signs of strength degradation after completion of all loading protocols. However, the braces exhibited significant cyclic strain hardening behavior —when compared to the carbon steel counterpart, the combined cyclic and strain hardening of the austenitic stainless steel braces was up to 52% larger.

3.4. Frames

Research on the inelastic behavior of structural stainless steel frames has shown that their behavior departs mildly from that traditionally assumed for carbon steel frames, in which idealized plastic hinges form at different locations until a collapse mechanism is reached. Structural stainless steel frames are better characterized by the formation of zones of plasticity with gradually reducing stiffness, but with peak capacities well in excess of the traditional plastic moment assumed for carbon steel frames (Walport et al.; 2019).

The feasibility of using structural stainless steels in moment frames (MF), concentrically braced frames (CBF) and eccentrically braced frames (EBF) has been studied by di Sarno et al. (2003; 2005; 2008) through pushover and nonlinear dynamic analyses on structural carbon steel and structural stainless steel frames. The numerical comparative study involved carbon steel frames and stainless steel frames of identical dimensions. All members of the structural stainless steel frames were modelled using a nonlinear stress-strain characteristic that resembled that of an austenitic stainless steel alloy, and with a yield strength equal to that of the carbon steel frame to facilitate the comparison. This study showed that using structural stainless steels for the SFRS can achieve equivalent or better seismic performance than carbon steel frames. The pushover analyses showed that, even though all frames had the same yield strength, once the frames started to deform plastically the structural stainless steel frames developed a consistently larger lateral resistance than the structural carbon steel frames. This was mostly due to the higher strain hardening exhibited by stainless steel. This difference in strain hardening exhibited by stainless steel also resulted in a different distribution of plasticity within the frame, which led to the concentration of inelastic deformations in some of the stainless steel MF at different locations from those in the geometrically equivalent carbon steel frame. It should be noted that these pushover analyses did not account for cyclic hardening, and therefore the response of the stainless steel frame to cyclic forces may differ from that predicted by the pushover analysis, with the concentration of inelastic deformation potentially occurring at different locations. As an example of the results obtained from these studies, Figure 14 compares the results from the pushover analyses on the CBF and EBF reported in di Sarno et al. (2008). These analyses revealed that the structural stainless steel frames (MF, CBF and EBF) exhibit an increase in overstrength of around 30% when compared to that of an equivalent frame made of carbon steel.

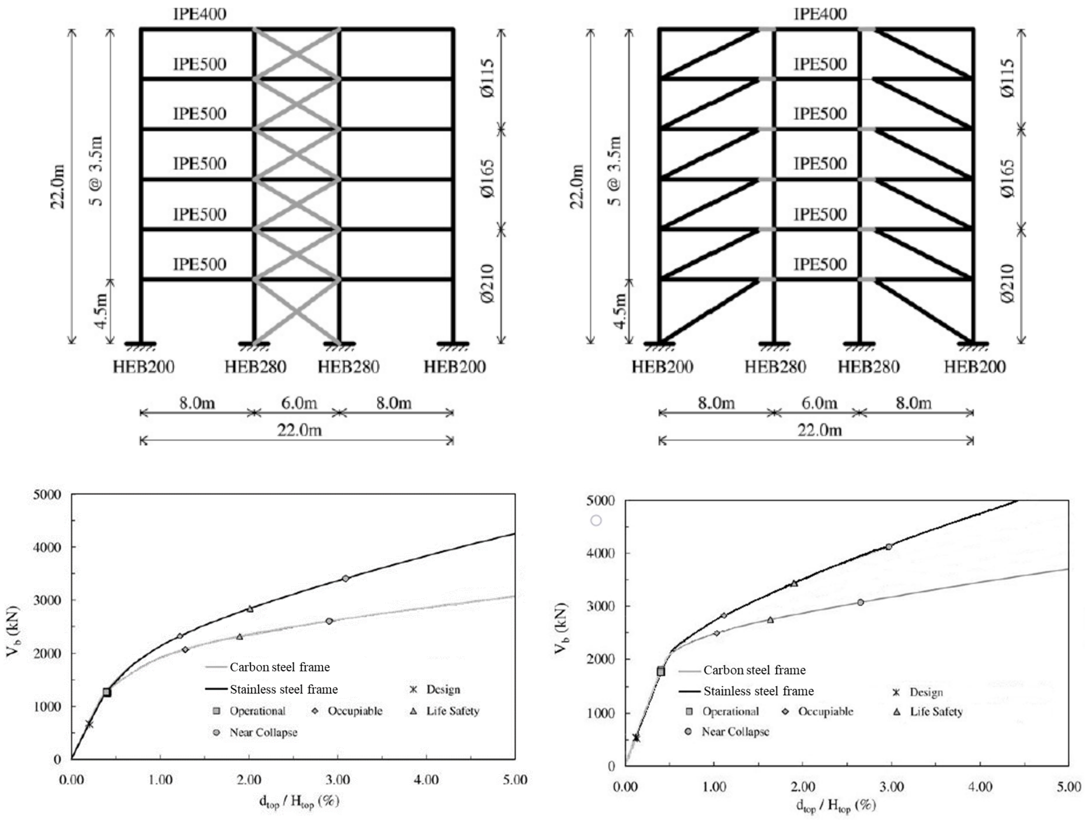

(a) (b)

Figure 14 Configuration of studied frames and results from pushover analyses: a) CBF; b) EBF (di Sarno et al., 2008).

4. RECOMMENDATIONS FOR U.S. SEISMIC DESIGN OF STAINLESS STEEL STRUCTURES

Given the available information, this section provides a recommendation for seismic design practice in the U.S., until such time as the standards can provide formal guidance. Inherent in these recommendations is that the engineer adheres to the structural stainless steel standard AISC 370 (AISC, 2021) in their design. Austenitic and duplex stainless steels in AISC 370 are able to meet the most stringent ductility requirements that are implicitly imposed by AISC 341 (AISC, 2022b) on carbon steel Grade 50. Further, structural stainless steel welded connections satisfy the most stringent CVN toughness requirements given in AWS D1.8/D1.8M (AWS, 2021) for 'demand critical' welds. Combined with the stable hysteretic behavior of austenitic and duplex stainless steel members experimentally demonstrated to date, it is concluded that the carbon steel seismic design rules are broadly applicable to structures with energy dissipating components made from austenitic or duplex stainless steel alloys if appropriate additions are made. Therefore, the primary guidance provided here is how the design and detailing requirements given in ASCE 7 (ASCE, 2022b) and AISC 341 could be modified to cover the seismic design of stainless steel structures.

4.1. Seismic design parameters (R, C_d and Ω_o)

For equivalent lateral force design per ASCE 7 (ASCE, 2022b) the seismic response modification coefficients R, C_d, and Ω_o are of paramount need for determining the seismic demands and estimated drift. Until further study is available, it is recommended that for structural stainless steel systems the same R be utilized as that of carbon steel, but the Ω_o and C_d be increased by a factor of 1.5, but not to exceed R. The logic behind these recommendations is provided in the following.

The response modification coefficient R depends on the structural overstrength and ductility of the system. At a material level, the ductility of stainless steel is equivalent to that of carbon steel, and therefore, provided the detailing requirement given in AISC 341 (AISC, 2022b) with the modifications highlighted in this paper are followed, a structural stainless steel SFRS should exhibit a ductility equivalent to or exceeding that of an equivalent carbon steel SFRS. As for the system overstrength Ω_o, this can be expected to be larger in a structural stainless steel SFRS due to the more pronounced strain hardening and cyclic hardening exhibited by the material. This suggests that an SFRS made of stainless steel could benefit from larger R-factors than those for carbon steel SFRS. However, given the lack of extensive system research and studies, and to provide an incentive for such future work, it is recommended to adopt the same R-factors that are prescribed in ASCE 7 for carbon steel SFRS.

System overstrength, Ω_o, depends on the overall system design, efficiency of member selection, and extent to which seismic design governs other portions of the structure. Comparing stainless steel systems to carbon steel systems the primary difference in overstrength is the impact of strain hardening in the static design, and cyclic hardening in the seismic response - both of which contribute to increased overstrength for stainless steel systems compared with carbon steel systems. The expected increase in overstrength is alloy and grade dependent, with austenitic stainless steels exhibiting a higher strain hardening modulus (E_{st}), and ratios F_u/F_y, and F_{cyc}/F_{mon} than duplex stainless steels. Increasing Ω_o by a factor of 1.5 is expected to be close to a mean response for large strain amplitudes in austenitic and an upperbound on duplex stainless steels —in the absence of more refined overstrength numbers this is recommended.

Seismic drift amplification, C_d, reflects additional drift amplification beyond elastic drift due to nonlinear system response. When compared with equivalent carbon steel structural systems, stainless steel systems may be expected to drift more before reaching extensive first yielding (due to the lower proportional limit and rounded stress-strain curve of stainless steel), but slightly less at large drifts due to higher levels of strain hardening and cyclic hardening. Use of a higher C_d results in higher system drift predictions and is generally considered more conservative. In the absence of definitive system studies, it is recommended to err on the side of caution and use a C_d amplified by a factor of 1.5 (but not to exceed R) to account for the initial softening.

Focusing on the structural systems most likely to be used in stainless steel, Table 3 and Table 4 implements these recommendation for SFRS of building and non-building structures, respectively. These modifications to the carbon steel seismic design parameters are conservative and based on judgement —research should be performed to remove all or some of this conservatism in the future.

Following the same rationale, the provisions in Chapter 13 of ASCE 7 can be applied to the design of nonstructural components in stainless steel SFRS provided the seismic loads on the nonstructural components and relative displacements are calculated using the recommended seismic design parameters for stainless steel SFRS.

Table 3 Recommended seismic design parameters for typical stainless steel building structures.

Type of structure		R	Ω_o	C_d
Moment frames	OMF	3.5	3.5	3.5
	IMF	4.5	4.5	4.5
	SMF	8	4.5	8
Concentrically braced frames	OCBF	3.25	3	3.25
	SCBF	6	3	6

Eccentrically braced frames	EBF	8	3	6
Buckling-restrained braced frames	BRBF	8	3.75	7.5
Note: OMF = Ordinary Moment Frame; IMF = Intermediate Moment Frame; SMF = Special Moment Frame; OCBF = Ordinary Concentrically Braced Frame; SCBF = Special Concentrically Braced Frame; EBF = Eccentrically Braced Frame; BRBF = Buckling-Restrained Braced Frame.				

Table 4 Recommended seismic design parameters for typical stainless steel nonbuilding structures.

Type of structure		***R***	**Ω_o**	**C_d**
Steel storage racks		4	3	4
Steel cantilever storage racks	OMF	2.5	2.5	2.5
	OBF	3.25	3	3.25
Building frame systems	OCBF	3.25	3	3.25
	SCBF	6	3	6
Moment-resisting frame systems	OMF	3.5	3.5	3.5
	IMF	4.5	4.5	4.5
	SMF	8	4.5	8
Trussed towers (freestanding or guyed)		3	3	3
Signs and billboards		3	2.7	3
Steel lighting system support pole structures		1.5	1.5	1.5
Note: OMF = Ordinary Moment Frame; IMF = Intermediate Moment Frame; SMF = Special Moment Frame; OCBF = Ordinary Concentrically Braced Frame; SCBF = Special Concentrically Braced Frame				

The provisions in ASCE 7 for structures assigned to Seismic Design Category (SDC) B or C, in which the structure is classified as a "steel system not specifically detailed for seismic resistance" (i.e. R = 3, Ω_o = 3, C_d = 3), are recommended to be extended to stainless steel structures except that the structure should be designed, fabricated, and erected in accordance with AISC 370. Available evidence indicates that material and system overstrength and ductility in stainless steel structures meets or exceeds carbon steel equivalents, so use of this provision is considered justified. Further, since $\Omega_o = C_d = R$ in these provisions, the drift and all capacity protected members are all at elastic levels. Similarly, the provisions in Chapter 15 of ASCE 7 for non-building structures for which design and detailing do not need to be in accordance with AISC 341, can also be extended to stainless steel structures. However, it should be noted that some types of carbon steel non-building structures, such as storage racks, or trussed towers, are designed based on specific industry standards for which there is no stainless steel equivalent.

4.2. Expected material strength

Fundamental to the use of AISC 341 (AISC, 2022b) for carbon steel seismic detailing requirements are the expected yield and tensile strength factors: R_y and R_t. AISC 341 utilizes R_y in width-to-thickness limits as well as in the expected strength of members and R_t in the expected strength of connections. These factors are specifically derived, based on material data collected for the carbon steel grades covered in that specification, and are therefore not applicable to stainless steels. Meza et al. (2024) provided updated material factors for structural stainless steels based on data from industry including the ratio of mean-to-nominal for the 0.2% offset yield stress, F_y, and the ultimate stress, F_u. These ratios are used directly for R_y and R_t in the carbon steel standard AISC 341, but as previously discussed stainless steel has additional overstrength due to higher levels of strain hardening and cyclic hardening which need to be accounted for in design. Two options are therefore considered in this paper: design option (1) is a simplified approach in which the effect of material overstrength, cyclic hardening and strain hardening are all combined in a single multiplicative factor $R_{y,comb}$; while design option (2) is presented as an alternative and more efficient design approach in which each effect is considered separately where needed. Table 5 provides the recommended R_y and R_t, where the statistical variation based on the mean overstrength ($F_{y,m}/F_y$) and the 95% fractile overstrength ($F_{y,95\%}/F_y$), cyclic hardening (F_{cyc}/F_{mon}), and strain hardening at different strain levels ($F_{1\%}/F_y$ and $F_{2\%}/F_y$) have all been separately approximated. For the material overstrength, given the wide variation shown by the data, which in the case of duplex stainless steels, displays a bi-modal distribution (see Figure 6), it is recommended to consider use of the 95% fractile (or similar choice) from the distribution. Further refinement of each factor in Table 5 based on alloy and grade are possible. As an alternative to the recommended overstrength values (i.e. $R_{y,95\%}$ and $R_{t,95\%}$), which could reduce the level of conservatism, these may be directly derived from tensile coupons extracted from structural components that are representative of those used for the energy-dissipating elements of the SFRS.

Table 5 Recommended expected material strength factors

	Austenitic	Duplex		Austenitic	Duplex
$R_{y,m} = F_{y,m}/F_y$ [a]	1.33	1.22	$R_{t,m} = F_{um}/F_u$ [a]	1.16	1.16
$R_{y,95\%} = F_{y,95\%}/F_y$ [a]	1.60	1.50	$R_{t,95\%} = F_{t,95\%}/F_y$ [a]	1.25	1.30
$R_{y,cyc} = F_{cyc}/F_{mon}$ [b]	1.60	1.50	$R_{t,cyc} = F_{cyc}/F_{mon}$ [b]	~1.1	~1.1
$R_{y,2\%} = F_{2\%}/F_y$ [c]	1.23	1.15			
$R_{y,1\%} = F_{1\%}/F_y$ [c]	1.15	1.10			
$R_{y,comb} = R_{y,95\%} \times R_{y,cyc} \times R_{y,2\%}$	3.15	2.59	$R_{t,comb} = R_{t,95\%} \times R_{t,cyc}$	1.38	1.43

[a] Meza et al. (2024), [b] Section 3.1 of this paper, [c] per AISC 370 Appendix 7, using Table 1 properties

Note, for cold-formed HSS the cold-forming process increases the average yield strength and this should be accounted for, either by (1) direct increase of F_y to $F_{y,avg}$ per AISC 370, or (2) additional increase in R_y based on $F_{y,avg}/F_y$ as calculated per AISC 370 for cold-formed HSS.

4.3. Expected member strength

AISC 341 (AISC, 2022b) generally utilizes R_yF_y in determination of the expected strength of a carbon steel member. For structural stainless steel members that follow the provisions of Chapters D to K of AISC 370 (AISC, 2021) this remains appropriate. AISC 370 Chapters D to K essentially adopt the elastic-plastic material model of carbon steel, appropriately corrected for stainless steel, in determination of member strength, and the R_y factors in Table 5 account for this approach appropriately.

However, Appendix 2 of AISC 370 also allows an alternative design method —the Continuous Strength Method (CSM), which allows the engineer to directly use the stainless stress-strain curve, or a close approximation, and integrate the resulting stress to determine member capacity. If utilizing this method, the expected strength should not include strain hardening, since it is implicitly included in the development of the member strength. For member strength determined by CSM, $R_{y,comb}$ of Table 5 should be divided by $R_{y,2\%}$ (i.e. ~1.23 for austenitic and ~1.15 for duplex stainless steel).

For cold-formed HSS (irrespective of whether they form part of the energy dissipating members or the protected members), the yield strength may be replaced by$F_{y,avg}$ when calculating the member strength, irrespective of whether the strength is calculated assuming the elastic-plastic material model or using the CSM, as indicated in AISC 370.

4.4. Capacity protected members and connections

Capacity protected members and connections are typically designed for the system seismic demands amplified to Ω_o levels or directly based on the expected strength (essentially R_yF_y) of the component delivering the demand. This philosophy is extended to structural stainless steel as long as the appropriate $\Omega_o$and R_y values are employed.

For capacity-based design, if the expected strength is determined following design option (1), the capacity-limited seismic load effect E_{cl} should be taken as $R_{y,comb}F_y$. However, if design option (2) is adopted, $R_{y,comb}F_y$ would only need to be used in those cases in which the energy dissipating member is expected to sustain excessive inelastic strains —in AISC 341 the equivalent expression for carbon steel is $1.1R_yF_y$, in which the 1.1 coefficient accounts for the combination of cyclic and strain hardening exhibited by the material. If the energy dissipating member is not expected to be subject to significant inelastic strains (reflected in AISC 341 by the use of R_yF_y in the calculation of E_{cl}), the expected strength of the member could be based on $R_{y,95\%}R_{y,1\%}F_y$.

4.5. Width-to-thickness requirements

Width-to-thickness requirements in AISC 341 (AISC, 2022b) are utilized for a variety of means —limit local buckling to provide ductility, limit cyclic strains to precent low-cycle fatigue, empirically align with tested members, etc. (Schafer et al. 2022). For stainless steel design per AISC 370 (AISC, 2021) Chapters D to K, it is recommended that the AISC 341 limits be utilized with the appropriately corrected R_y factors. If design option (1) is adopted to predict the expected strength, all width-to-thickness limits should be calculated using $R_{y,comb}F_y$. However, if design option (2) is followed, only the width-to-thickness limits for highly ductile members (λ_{hd}) should be based on $R_{y,comb}$, while for moderately ductile members (λ_{md}) the expected strength may be based on $R_{y,95\%}R_{y,1\%}F_y$, as in this case the member is not expected to be subject to large strains. Evidence exists in the literature that in some cases both approaches may be conservative (see e.g. Gonzalez de Leon et al. 2022 as previously discussed). This is in part because the use of R_y factors to account for strain hardening and cyclic hardening increases the assumed slenderness of the element —while in reality the stainless steel element may have higher strain hardening stiffness and be less prone to local buckling. Use of different R_y factors for expected member strength and width-to-thickness may be justified in the future for stainless steel; currently insufficient research exists to fully implement such a change.

For those that use CSM in AISC 370, width-to-thickness limits are not utilized, as the method utilizes strain limits instead. The width-to-thickness limits in AISC 341 for moderately and highly ductile members target a strain of around $4\varepsilon_y$ and $15\text{-}20\varepsilon_y$, respectively (Schafer et al.; 2020, 2022). Specific strain limits may be back-calculated per Schafer et al. (2022) and utilized in CSM-based design. One convenience for CSM-based design is that where the maximum story drift is known, it may be converted into a required strain demand and this demand utilized in performing CSM checks.

4.6. Stability bracing requirements

Extension of AISC 341 (AISC, 2022b) to stainless steel is in many cases straightforward: use the updated R_y factor based on the design option adopted (i.e. design option 1 or 2), and follow the standard. However, in other cases AISC 341 may utilize derived forms of AISC 360 (AISC, 2022a) that are slightly different for carbon and stainless steel in AISC 370 (AISC, 2021). A prominent example are the stability bracing requirements for highly and moderately ductile members, as well as those for special braces.

4.6.1. Spacing

For SFRS made of carbon steel, the maximum spacing for the stability braces of highly ductile members given in AISC 341 was derived from the expression given in AISC 360 —reproduced here in Equation 1, where M_2 is the largest moment at the ends of the unbraced length, and M_1' is the effective moment at the opposite end from M_2.

$$L_b = \left(0.12 - 0.076\frac{M_1'}{M_2}\right)\frac{E}{F_y}r_y \tag{1}$$

Under seismic action the beam of the SFRS is generally expected to be subject to reverse curvature, with the moment at both ends reaching the plastic moment. However, due to uncertainties regarding the exact location of the inflection point during an earthquake, and for simplicity, AISC 341 conservatively assumes that the beam is in single curvature within the unbraced length, with one end of the beam reaching its plastic moment and the other end subject to half of that moment. Therefore, replacing the ratio M_1'/M_2 in Equation 1 with 0.5 and replacing the specified minimum yield strength with the expected yield strength (R_yF_y), the AISC 341 equation for calculating the maximum spacing for the stability braces in highly ductile members is obtained, as given by Equation 2.

$$L_b = (0.12 - 0.076 \times 0.5)\frac{E}{R_yF_y}r_y \backsimeq 0.086\frac{E}{R_yF_y}r_y \qquad (2)$$

For moderately ductile beams, because the inelastic demand is half of that for highly ductile beams, AISC 341 sets the maximum spacing for the stability braces as twice of that given by Equation 2.

AISC 370 includes an equivalent expression to Equation 1 for stainless steel reproduced here as Equation 3:

$$L_b = \left(1.83 - 1.17\frac{M_1'}{M_2}\right)L_p \qquad (3)$$

where L_p is given in AISC 370 and takes different values for austenitic and duplex stainless steel I-section beams. Following the same approach used for carbon steel, the maximum spacing for the stability braces of stainless steel beams designed as highly ductile members can be derived, as given by Equation 4 or 5 depending on whether design option (1) or (2) is adopted.

$$L_b = \frac{1.25L_p}{\sqrt{R_{y,comb}F_y}} \qquad \text{For design option 1} \qquad (4)$$

$$L_b = \frac{1.25L_p}{\sqrt{R_{y,95\%}R_{y,1\%}F_y}} \qquad \text{For design option 2} \qquad (5)$$

For moderately ductile stainless steel beams, the maximum spacing for the stability braces is assumed to be twice that for highly ductile beams, same as in carbon steel.

The brace spacing adjacent to special braces should be determined using Equation 4 irrespective of the design option adopted.

4.6.2. Strength and stiffness requirements

Strength and stiffness requirement are recommended to follow the approach of AISC 341 (AISC, 2022b), but utilizing the AISC 370 (AISC, 2021) bracing provisions instead of AISC 360 (AISC, 2022a). The stiffness requirements given in AISC 370 are the same as those in AISC 360 for carbon steel braces, but the strength requirements are 50% higher. AISC 341 specifies that the strength and stiffness requirements of the stability bracing in moderately and highly ductile beams should be satisfied assuming the braced beam reaches its expected plastic moment capacity (i.e. $M_r = R_yF_yZ/\alpha_s$, where α_s is the LRFD-ASD force level adjustment factor). This approach is applicable to stainless steel stability braces only when the braced beam is designed without consideration of strain hardening (i.e. per AISC 370 Chapter F). In this is the case, the expected plastic moment capacity should be based on $R_{y,comb}F_y$ if design option (1) is adopted, and $R_{y,95\%}R_{y,1\%}F_y$ if design option (2) is adopted.

If the braced beam is designed using CSM, the R_y factor used in the calculation of the required flexural strength of the beam should not considering the component due to static strain hardening to avoid double counting for this effect. Therefore, if design option (1) is adopted, $R_{y,comb}$ of Table 5 should be divided by $R_{y,2\%}$ (i.e. ~1.23 for austenitic and ~1.15 for duplex stainless steel) and $F_y Z$ replaced with the CSM flexural strength. If design option (2) is adopted, the expected CSM flexural strength should be determined based on $R_{y,95\%}F_y$.

For the special braces that have to be placed near the expected location of plastic hinges in IMF, SMF and EBF, the expected moment capacity should be based on $R_{y,comb}F_y$ irrespective of whether design option (1) or (2) are adopted, unless the member capacity is determined using CSM, in which case $R_{y,comb}$ should be divided by $R_{y,2\%}$.

4.7. Nonlinear response history analysis

The seismic design of a structural stainless steel system may be based on a nonlinear response history analysis (NLRHA) in accordance with Chapter 16 of ASCE 7 (ASCE, 2022b). This approach avoids the use of the conservative seismic design parameters recommended in Section 4.1 and assumptions regarding the cyclic hardening behavior of the energy dissipating elements of the SFRS, resulting in a more efficient solution. Seismic design based on a NLRHA can also be beneficial for SFRS in which structural stainless steel is used in combination with carbon steel, or in which austenitic and duplex stainless steels are combined. In these cases, the cyclic hardening behavior of the different energy dissipating elements may differ significantly, and the choice of seismic design parameters may require the adoption of conservative assumptions. If the seismic design is based on a NLRHA, ASCE 7 still requires that a linear analysis in accordance with any of the procedures given in Chapter 12 of ASCE 7 should be performed to ensure that the structure meets the minimum strength and other criteria achieved with these linear analysis procedures. However, in this case, ASCE 7 permits to take the value of Ω_o as 1.0 because the seismic demands required for the design of critical elements are more accurately determined through the NLRHA. It should be noted, however, that in order to perform a NLRHA, the structural model should incorporate an accurate representation of the nonlinear stress-strain characteristic of stainless steels, which can be achieved using the Ramberg-Osgood material model given in AISC 370 (AISC, 2021). The structural model should also be able to capture the cyclic hardening behavior of stainless steel. This can be achieved by carrying out cyclic material tests of small coupons extracted from structural components that are representative of those used for the energy-dissipating elements of the SFRS or using available experimental data. In general NLRHA for structural stainless steel systems is encouraged; however, the information required for accurate modeling is substantial, and it is expected that its use will remain limited until such time as more direct modeling guidance is provided to engineers.

5. FURTHER RESEARCH NEEDS

While Section 4 has outlined preliminary recommendations for how the design and detailing requirements given in ASCE 7 (ASCE, 2022b) and AISC 341 (AISC, 2022b) could be modified to cover the design of structural stainless steel SFRS, there are a number of design considerations that require further research in order to develop comprehensive seismic design and detailing requirements for stainless steel structures. These include the following:

- Further refinement of R_y and R_t factors for calculating the expected strength of austenitic and duplex stainless steels, including potential separation of variance and strain hardening.
- Detailed characterization of the cyclic hardening behavior of austenitic and duplex stainless steel, including the effect that different product forms and the level of cyclic strain may have on this phenomenon. Consideration of expected and lowerbound characterizations of cyclic hardening for use in seismic design.

- Extensions for the use of CSM in NLHRA similar to recent guidance provided for nonlinear static analysis of frames by CSM.
- Development of system archetypes and formal FEMA P695 (FEMA, 2009) development of seismic response modification coefficients for structural stainless steel systems.
- Further refinement of expected strength and capacity-based design provisions for stainless steel members with strain hardening and cyclic hardening.
- Development and/or extension of pre-qualified connections for structural stainless steel.
- Development of hybrid details such that stainless steel may be incorporated in a carbon steel system (e.g. as an EBF) as the energy dissipating element and still meet 'demand critical' weld criteria. Also, further work on the suitability of bolted connections between dissimilar metals in an SFRS is needed.

6. Conclusions

This study underscores the need for dedicated seismic design standards for structural stainless steel, particularly for seismic force resisting systems in high seismic regions. Key findings demonstrate that the unique material properties of austenitic and duplex stainless steels —such as significant strain hardening, ductility, and cyclic toughness— offer potential advantages over traditional carbon steel in seismic applications, but also require modifications to traditional design. The lack of established design rules hinders wider adoption of structural stainless steel.

Preliminary recommendations for extending current seismic design provisions, including modifications to ASCE 7 and AISC 341, provide a foundation for incorporating stainless steel into seismic force-resisting systems. These include proposed seismic response modification coefficients for equivalent lateral force-based design, and tailored material and member expected strength provisions to account for the expected performance of stainless steel systems. The recommendations provide a complete design approach, but are intentionally conservative in many instances due to insufficient knowledge or insufficient research to justify more precise procedures.

Future research is essential to expand and validate these recommendations, particularly regarding the cyclic hardening characteristics, low-cycle fatigue behavior, and capacity-based design approaches for stainless steel. Additionally, experimental studies are needed to refine seismic design parameters and evaluate the integration of stainless steel components within hybrid systems. With these advancements, structural stainless steel can emerge as a resilient and efficient material for seismic applications, aligning with global performance and sustainability objectives.

REFERENCES

AISC, 2016. Specification for Structural Steel Buildings, AISC 360-16, American Institute of Steel Construction, Chicago, Ill.

AISC, 2021. Specification for Structural Stainless Steel Buildings, AISC 370-21, American Institute of Steel Construction, Chicago, Ill.

AISC, 2022a. Specification for Structural Steel Buildings, AISC 360-22, American Institute of Steel Construction, Chicago, Ill.

AISC, 2022b. Seismic Provisions for Structural Steel Buildings, AISC 341-22, American Institute of Steel Construction, Chicago, Ill.

AISC, 2022c. Prequalified Connections for Special and Intermediate Steel Moment Frames for Seismic Applications, AISC 358-22, American Institute of Steel Construction, Chicago, Ill.

Annan, C-D. and Beaumont, E. (2020) "Low-cycle fatigue of stainless steel plates under large plastic strain demands", Journal of Building Engineering, Vol. 29, 101160.

ASCE, 2022a. Specification for the Design of Cold-Formed Stainless Steel Structural Members, 2022 Edition (ASCE8-22), American Society of Civil Engineers, Reston, VA.

ASCE, 2022b. Minimum Design Loads and Associated Criteria for Buildings and Other Structures, 2022 Edition (ASCE7-22), American Society of Civil Engineers, Reston, VA.

AWS, 2017. Structural Welding Code—Stainless Steel, AWS D1.6/D1.6M:2017, American Welding Society, Miami, Fla.

AWS, 2020. Structural Welding Code—Steel, AWS D1.1/D1.1M:2020, American Welding Society, Miami, Fla.

AWS, 2021. Structural Welding Code—Seismic Supplement, AWS D1.8/D1.8M:2021, American Welding Society, Miami, Fla.

Baddoo, N.R., 2013. Structural Stainless Steel, Design Guide 27,1st Ed., AISC, Chicago, Ill.

Baddoo, N.R. and Meza, F.J., 2022. Structural Stainless Steel, Design Guide 27, 2nd Ed., AISC, Chicago, Ill.

Baiguera, M., Vasdravellis, G. and Karavasilis, T.L., 2019. "Ultralow Cycle Fatigue Tests and Fracture Prediction Models for Duplex Stainless-Steel Devices of High Seismic Performance Braced Frames", Journal of Structural Engineering (ASCE), Vol. 145(1), 04018230.

CEN, 2004. Design of structures for earthquake resistance – Part 1: General rules, seismic actions and rules for buildings EN 1998-1, European Standard, Brussels.

CEN, 2015. Design of steel structures – Part 1-4: General rules – Supplementary rules for stainless steel EN 1993-1-4, European Standard, Brussels.

Chang, X., Yang, L., Zong, L., Zhao, M.H. and Yin, F., 2019. "Study on cyclic constitutive model and ultra low cycle fracture prediction model of duplex stainless steel", Journal of Constructional Steel Research, Vol. 152, pp. 105-116.

CECS, 2015. Technical specification for stainless steel structures CECS 410, China Engineering Construction Standardization Association Light Steel Structure Committee

Di Sarno, L., Elnashai, A.S. and Nethercot, D.A., 2003. "Seismic performance assessment of stainless steel frames", Journal of Constructional Steel Research, Vol. 59, 1289-1319.

Di Sarno, L., Elnashai, A.S. and Nethercot, D.A., 2005. "Seismic retrofitting of framed structures with stainless steel", Journal of Constructional Steel Research, Vol. 62, pp. 93-104.

Di Sarno, L., Elnashai, A.S. and Nethercot, D.A., 2008. "Seismic response of stainless steel braced frames", Journal of Constructional Steel Research, Vol. 64, pp. 914-925.

Dutta, A., Dhar, S. and Acharyya, S.K., 2010. "Material characterization of SS 316 in low-cycle fatigue loading", Journal of Materials Science, Vol. 45, pp. 1782-1789.

ECCS, 1986. Recommended testing procedure for assessing the behaviour of structural steel elements under cyclic loads, Brussels.

Federal Emergency Management Agency (FEMA), 2009. Qualification of building seismic performance factors, FEMA P695, Washington, D.C

Gonzalez de Leon, I., Nastri, E., Arrayago, I., Montuori, R., Piluso, V. and Real, E., 2022. "Experimental study on stainless steel tubular members under cyclic loading", Thin-Walled Structures, Vol. 181, 109969.

GB, 2010. Code for seismic design of buildings GB 50011-2010, National Standard of the People's Republic of China, Beijing.

Kim, R.H, Kim, T.S., Im, S.H. and Xi, Y., 2021. Hysteretic behavior comparison of austenitic and lean duplex stainless steel square hollow section members under cyclic axial loading, Engineering Structures, Vol. 237, 112227.

Lanning, J., Benzoni, G. and Uang, C-M., 2016. “Using buckling-restrained braces on long-span bridges. I: Full-scale testing and design implications, Journal of Bridge Engineering (ASCE), 04016001.

Lazaro, L. and Chacon, R., 2022. “Material behaviour of austenitic stainless steel subjected to cyclic and arbitrary loading”, Journal of Constructional Steel Research, Vol. 189, 107113.

Meza, F.J., Baddoo, N. and Gardner, L., 2024. “Derivation of stainless steel material factors for European and U.S. design standards”, Journal of Constructional Steel Research, Vol. 213, 108383.

Nip, K.H., Gardner, L., Davies, C.M. and Elghazouli, A.Y., 2010a. “Extremely low cycle fatigue tests on structural carbon steel and stainless steel”, Journal of Constructional Steel Research, Vol. 66, pp. 66-110.

Nip, K.H., Gardner, L. and Elghazouli, A.Y., 2010b. “Cyclic testing and numerical modelling of carbon steel and stainless steel tubular bracing members”, Engineering Structures, Vol. 32, pp. 424-441.

Schafer, B.W., Fraser, T. Goel, S., McManus, P., Sherman, D., Sabol, T., Uang, C.-M., and Varma, A. 2020. “Task Group Report on Local Buckling (Width-to-Thickness) Limits,” prepared by the AISC Committee on Specifications Ad Hoc Task Group on Local Buckling (Width-to-Thickness) Limits, January 7, AISC, Chicago, Ill.

Schafer, B.W., Geschwidner, L.F., Sabol, T. and Uang, C-M. 2022. “Review of local buckling width-to-thickness limits”, Engineering Journal, American Institute of Steel Construction, Vol. 59, pp. 65-84.

Tada, M., Fukui, T., Nakashima, M. and Roeder, C.W., 2003. “Comparison of strength capacity for steel building structures in the United States and Japan”, Earthquake Engineering and Engineering Seismology, Vol. 4(1), pp. 37-49.

Voestalpine, 2013. “Filler Metals Bestseller for Joining Applications,” Voestalpine Böhler Welding, Austria.

Walport, F., Gardner, L., Real, E., Arrayago, I. and Nethercot, D.A., 2019. “Effects of material nonlinearity on the global analysis and stability of stainless steel frames”, Journal of Constructional Steel Research, Vol. 152, pp. 173-182.

Wang, Y.Q., Chang, T., Shi, Y.J., Yuan, H.X., Yang, L. and Liao, D.F., 2014. “Experimental study on the constitutive relation of austenitic stainless steel S31608 under monotonic and cyclic loading”, Thin-Walled Structures, Vol. 83, pp. 19-27.

Yin, F., Yang, L., Wang, M., Zong, L. and Chang, X., 2019. “Study on ultra-low cycle fatigue behavior of austenitic stainless steel”, Thin-Walled Structures, Vol. 143, 106205.

Zhou, F. and Li, L., 2016. “Experimental study on hysteretic behaviour of structural stainless steels under cyclic loading”, Journal of Constructional Steel Research, Vol. 122, pp. 94-109.

Zhou, F., Fang, C. and Chen, Y., 2018. “Experimental and numerical studies on stainless steel tubular members under axial cyclic loading”, Engineering Structures, Vol. 171, pp. 72-85.